The Soil Moisture–Atmosphere Coupling Experiment (SMACEX): Background, Hydrometeorological Conditions, and Preliminary Findings

WILLIAM P. KUSTAS

Hydrology and Remote Sensing Laboratory, ARS, USDA, Beltsville, Maryland

JERRY L. HATFIELD AND JOHN H. PRUEGER

National Soil Tilth Laboratory, ARS, USDA, Ames, Iowa

(Manuscript received 1 May 2004, in final form 4 February 2005)

ABSTRACT

The Soil Moisture–Atmosphere Coupling Experiment (SMACEX) was conducted in conjunction with the Soil Moisture Experiment 2002 (SMEX02) during June and July 2002 near Ames, Iowa—a corn and soybean production region. The primary objective of SMEX02 was the validation of microwave soil moisture retrieval algorithms for existing and new prototype satellite microwave sensor systems under rapidly changing crop biomass conditions. The SMACEX study was designed to provide direct measurement/remote sensing/modeling approaches for understanding the impact of spatial and temporal variability in vegetation cover, soil moisture, and other land surface states on turbulent flux exchange with the atmosphere. The unique dataset consisting of in situ and aircraft measurements of atmospheric, vegetation, and soil properties and fluxes allows for a detailed and rigorous analysis, and the validation of surface states and fluxes being *diagnosed* using remote sensing methods at various scales. Research results presented in this special issue have illuminated the potential of satellite remote sensing algorithms for soil moisture retrieval, land surface flux estimation, and the assimilation of surface states and diagnostically modeled fluxes into prognostic land surface models. Ground- and aircraft-based remote sensing of the land surface and atmospheric boundary layer properties are used to quantify heat fluxes at the tower footprint and regional scales. Tower- and aircraft-based heat and momentum fluxes are used to evaluate local and regional roughness. The spatial and temporal variations in water, energy, and carbon fluxes from the tower network and aircraft under changing vegetation cover and soil moisture conditions are evaluated. An overview of the experimental site, design, data, hydrometeorological conditions, and results is presented in this introduction, and serves as a preface to this special issue highlighting the SMACEX results.

1. Introduction

The Soil Moisture–Atmosphere Coupling Experiment (SMACEX) was designed to provide a multiscale dataset of vegetation, soil, and atmospheric states, representing a mixture of point, linear, and gridded coverage. The SMACEX campaign overlapped with the Soil Moisture Experiment 2002 (SMEX02), whose primary objectives were to extend microwave soil moisture observations and retrieval algorithms to rapidly changing crop biomass conditions, to acquire data required for validating the Earth Observing System (EOS) *Aqua* Advanced Microwave Scanning Radiometer (AMSR)-E brightness temperatures and soil moisture retrieval algorithms, and to evaluate new soil moisture sensing instruments (Njoku et al. 2004). Ultimately, the soil moisture maps that are generated from the various sensors will provide a key boundary condition for land surface modeling.

The data from SMACEX and SMEX02 will be used to address several scientific research topics/issues related to land surface–atmosphere dynamics. These include 1) the evaluation of spatial scaling techniques and assumptions inherent in turbulent transport modeling, 2) the direct evaluation of the role of the spatial and temporal variability in soil moisture and vegetation conditions on soil–vegetation–atmosphere interactions and on local- and regional-scale fluxes, and 3) the exploration of opportunities for assimilating remote sens-

Corresponding author address: William P. Kustas, USDA-ARS, Hydrology and Remote Sensing Lab, Bldg. 007, BARC-WEST, Beltsville, MD 20705.
E-mail: bkustas@hydrolab.arsusda.gov

ing products in order to improve land surface process modeling.

Results of this research will lead to a greater understanding of the role of soil moisture and vegetation conditions on planetary boundary layer dynamics for this region, and an assessment of the utility of remote sensing data for improving coupled land–atmosphere models. This, in turn, will lead to more reliable weather forecasting and regional climate predictions. More specifically, the data and research results will assist in substantiating a growing body of evidence from model simulations that suggest that agricultural practices can modify the local and regional climate (Adegoke et al. 2003; Weaver and Avissar 2001).

More immediate impacts from the SMACEX project will come from research results evaluating the significance of soil moisture/soil texture differences, phenological differences between the two main agricultural crops, and differences in management practices (i.e., conventional till, no till, ridge till, row spacing) on the land surface energy exchanges across this landscape. Moreover, as a result of the partial canopy coverage during crop development and varying crop and tillage practices, which includes row spacing and orientation, crop cover is not uniform. Consequently, the interpretation of remotely sensed data (including thermal-infrared data and vegetation indexes), and the subsequent estimation of soil and vegetation energy exchanges, will be affected. The significance of these effects on land surface model output at the canopy, field, and regional scales will be addressed with the SMACEX dataset.

This preface paper describes the study site in Iowa, the experimental design and measurement activities, and the vegetation, soil, and hydrometeorological conditions that existed during the SMACEX field campaign. This will be followed by a summary of the major findings that are being presented in this special issue. Implications of these results on the specific research areas described above will be discussed.

2. Site description and experiment design

a. Site description

The SMACEX study site, a grid box ~ 10 km north–south by 30 km east–west, encompassed the Walnut Creek (WC) watershed (centered at 41.96°N, 93.6°W), which has been intensively monitored by the U.S. Department of Agriculture (USDA) Agricultural Research Service (ARS) National Soil Tilth Laboratory (NSTL) since 1990 as a field/watershed study site (Hatfield et al. 1999b). This WC experimental domain was nested within a regional (Iowa, hereafter IA) study area (~95 km north–south × 40 km east–west) that is used by SMEX02 to encompass several AMSR-E pixels (Fig. 1).

The land cover in the WC study area is primarily comprised of corn- (*Zea mays* L.) and soybean [*Glycine max* (L.) Merr.] fields. A land use map generated for the site indicates that nearly 95% of the region is in corn and soybean production, with the remaining land cover being comprised of cereal crops, urban areas/roads/farmsteads, forested/riparian areas, and lakes/rivers (Fig. 2). The typical field size is on the order of 25 ha, but ranges from ~1 to 130 ha. Although the WC watershed covers a relatively small area (~5100 ha), it contains all land cover types representing WC and IA experimental domains. In fact, even the WC and IA experimental domains are relatively small compared to the regional climate scale, however, both have topography and soil that are representative of the Des Moines lobe (Fig. 1), which covers approximately 1/4 of the state of Iowa (Hatfield et al. 1999b). Moreover, the corn and soybean production in this part of the state is indicative of a much larger agricultural region, namely, the upper Midwest corn–soybean region of the United States, which comprises over 60 million ha and represents 60% of all U.S. cultivated cropland.

The climate in this region is humid, with an average annual rainfall of 835 mm. In a typical growing season, the most rapid growth in corn and soybean crops is observed in the months of June and July, with corn biomass reaching 3–4 kg m^{-2}, while there can be a soybean biomass of 1–2 kg m^{-2}. This translates to leaf area index (LAI) values (by definition, one sided) for corn on the order of four and two for soybean, with both crops completely covering the soil surface.

Rainfall events in the spring and summer are often thunderstorms, providing brief and intense showers (Hatfield et al. 1999a). A rain gauge network in and around the watershed monitored by NSTL indicates that the heaviest precipitation months are May and June (about 1/3 of the annual total). The topography is characterized by low relief and poor surface drainage. Nearly 75% of the watershed is essentially flat, except for the "prairie potholes," while the remaining 25% contains more topographic relief and more dissected streams, and has better drainage. The soils are clay and silty clay loams, with generally low permeability (Hatfield et al. 1999b). A soils map for the WC region (Fig. 3) indicates that sandier soils are located near tributaries and in the eastern end, but in most other areas the soil texture is fairly uniform.

Anthropogenic forces have significantly modified the hydrologic character of the basin. Over the past 100 yr,

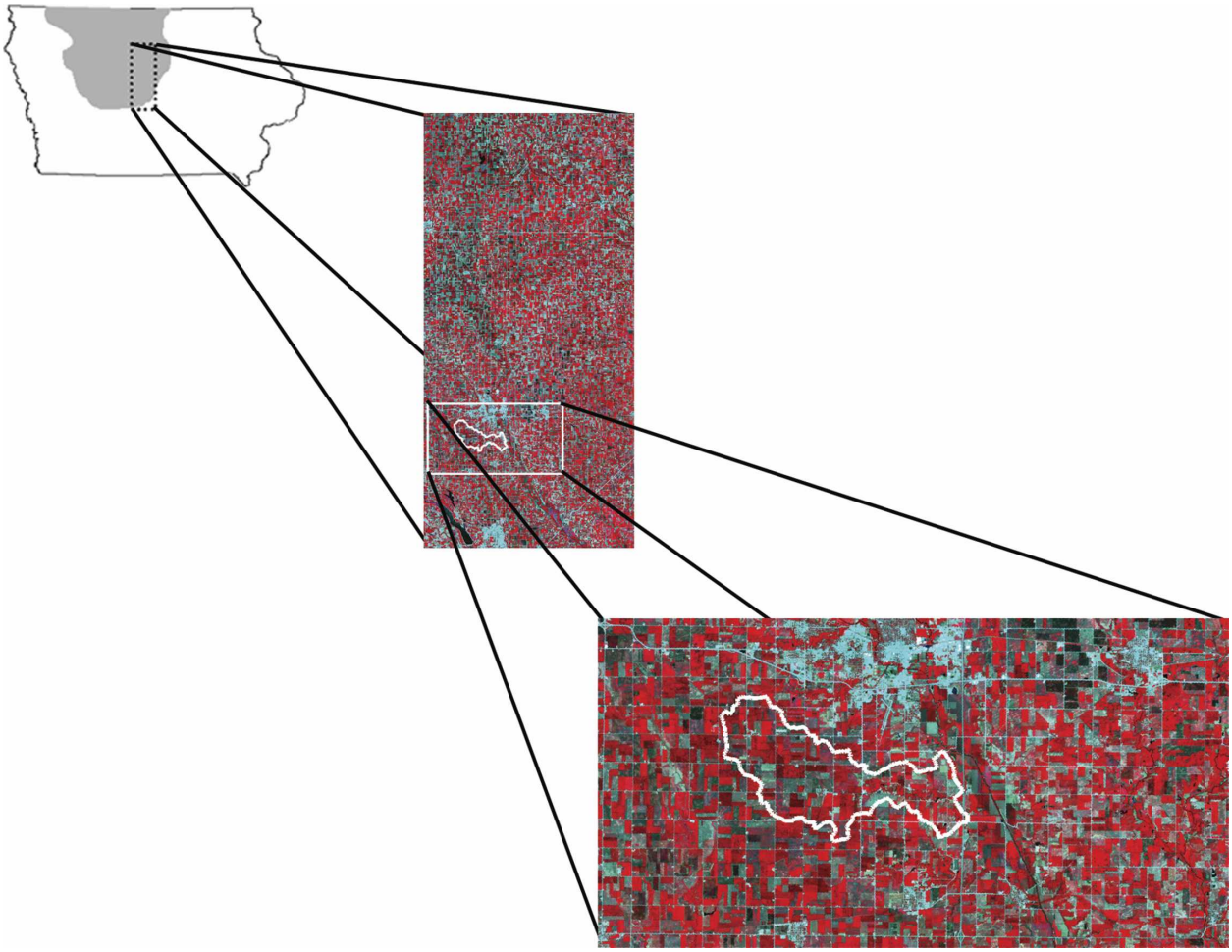

FIG. 1. The SMACEX (WC) and SMEX02 (IA) experimental domains within the state of Iowa from a *Landsat-7* enhanced Thematic Mapper (ETM) false-color image. The WC watershed boundary is delineated in white. These study sites have soils and topography representative of the Des Moines lobe (shaded area in the state map).

most of the prairie potholes have been drained, much of the land cultivated, and many of the agricultural fields tile drained to assist in subsurface drainage (tile flow). Conventional tillage is most widely used, however, no tillage and ridge tillage have been recently introduced.

Longer-term hydrometeorological observations that are collected and processed by the NSTL include 20 recording rain gauges, which also have mounted screen-level air temperature sensors placed in a grid pattern throughout the watershed (Fig. 4). Two meteorological stations are located in the watershed and record air temperature, relative humidity, wind speed and direction, soil temperature, and solar radiation. Five stream-gauging locations in the watershed are designed to isolate water flow and water quality for three subwatersheds and the entire basin (Hatfield et al. 1999b).

b. Experiment design

The intensive measurement campaign for SMACEX mainly covered the period from 15 June [day of year (DOY) 166] through 8 July (DOY 189). During this period, remote sensing data were collected from ground, aircraft, and satellite platforms. The SMEX02 campaign started later, on 25 June (DOY 176), and ended on 12 July (DOY 193). During the overlap of the two field campaigns, the vegetation grew rapidly and surface soil moisture changed from dry to wet from rainfall events in early July.

The WC study area was the focus of SMACEX measurement activities, as well as extensive vegetation and soil moisture sampling for SMEX02 of the over 30 field sites (Fig. 4). A major part of SMACEX involved measurements of surface energy, water, and carbon fluxes,

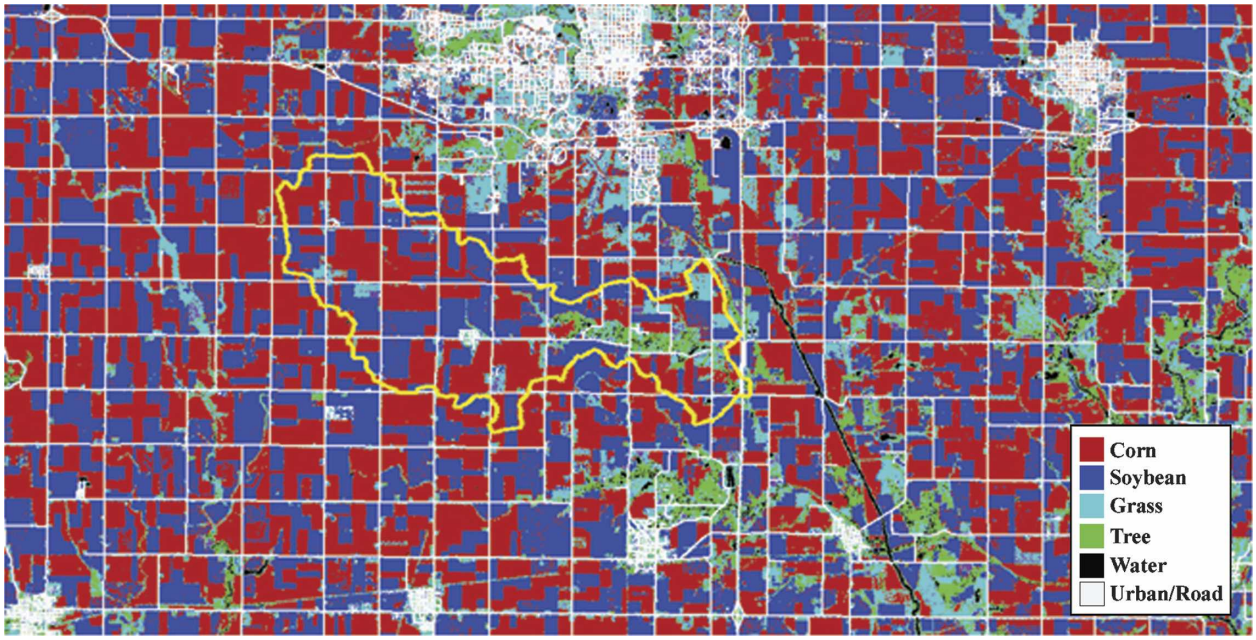

FIG. 2. Land use map of the WC study area with the city of Ames, IA, to the north. The WC watershed boundary is delineated in yellow.

as well as mean and turbulent atmospheric boundary layer (ABL) properties, and the collection of very high resolution visible, near-infrared, and thermal-infrared remote sensing imagery. The measurements are briefly described below, with more detailed information provided in the next section. In Table 1, a summary of the frequency and duration of measurements in support of SMACEX is provided.

Central to the SMACEX measurement activities was the deployment of meteorological-flux (METFLUX) towers employing eddy covariance (EC) at 12 field sites (6 corn and 6 soybean) distributed throughout the WC

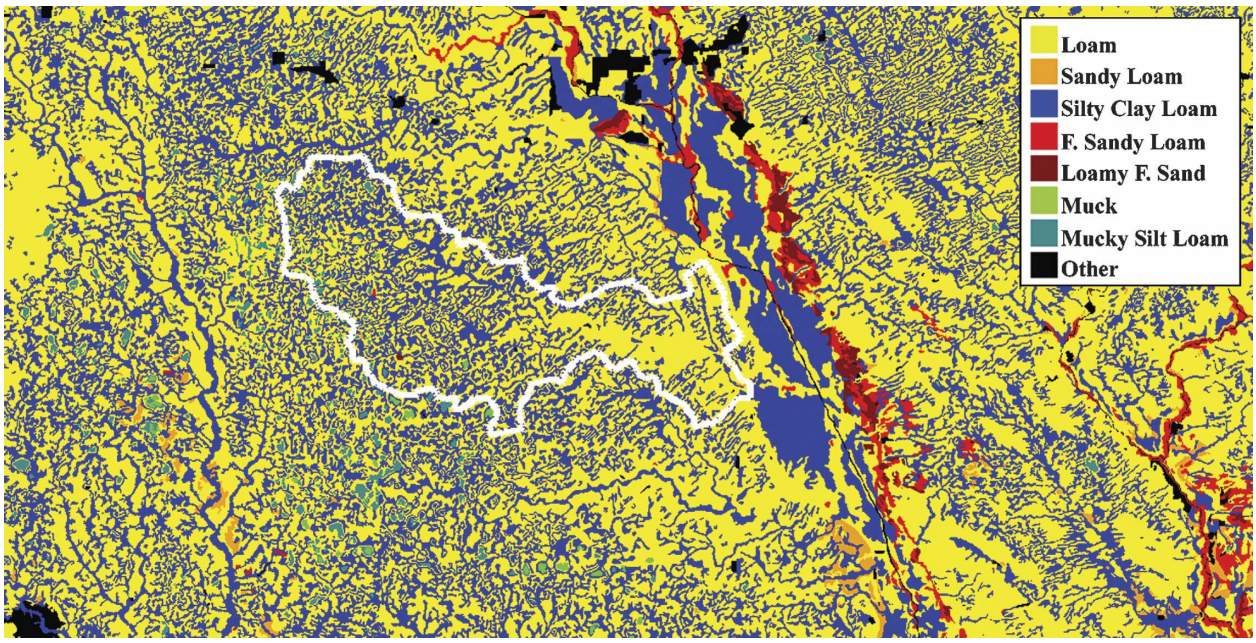

FIG. 3. Soil texture map for the WC experimental domain. The WC watershed boundary is delineated in white.

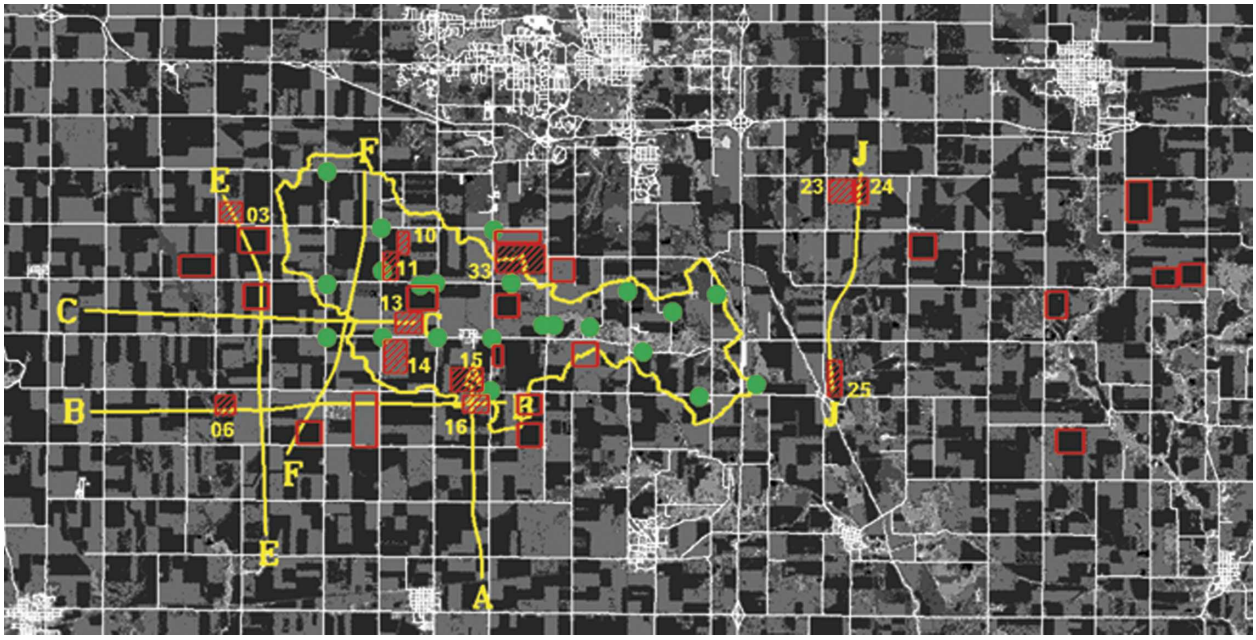

FIG. 4. Within the WC study area, the location of field sampling sites for soil moisture, vegetation cover/biomass (red rectangles), fields (numbered) with METFLUX towers (hashed rectangles), rain gauges (green solid circles), Twin Otter flux aircraft transects (yellow lines), labeled A, B, C, E, F, and J, and the WC boundary (delineated in yellow).

study area (Fig. 4). The towers were instrumented with sensors for measuring turbulent fluxes of water vapor and sensible heat, as well as net radiation and soil heat flux, with a subset measuring carbon dioxide flux. Additional hydrometeorological observations included wind speed and direction, air temperature, vapor pressure, near-surface soil temperature and moisture, and below- and above-canopy radiometric surface temperature.

At one site, a ground-based light detection and ranging (lidar) system from the Los Alamos National Laboratory (LANL) and the University of Iowa (UI), measuring ABL water vapor, height, and cloud cover and properties, was placed at the boundary between a corn- and soybean field (Fig. 4). Atmospheric radiosoundings and acoustic sonic detection and ranging (sodar) soundings were also collected at this location, providing ABL profiles of wind speed and direction, virtual temperature, and humidity.

The National Research Council of Canada Twin Otter atmospheric research aircraft flew transects over the WC study area that were designed to intersect several of the METFLUX tower stations and to be used as a means of estimating large-scale momentum, water, energy, and carbon fluxes (Fig. 4). Fluxes were measured at approximately 40 m AGL on repeated passes over six tracks ranging in length from 6 to 12 km. Most flights included at least two soundings, which provided atmospheric profiles from about 20 m AGL to about 300 m above the top of the mixed layer.

Very high resolution visible, near-infrared, and thermal-infrared imagery were collected over the WC study area using a remote sensing system that was designed at and flown by the Remote Sensing Services Laboratory at Utah State University (USU), mounted in a light twin-engine Piper Seneca II. Missions included mapping the WC experimental domain at ~3300 m AGL

TABLE 1. A summary of measurements conducted in direct support of the SMACEX field campaign.

Measurement source	Dates of observation	Time period (CST) or frequency	Specific days (DOY)
METFLUX towers	15 Jun–8 Jul	Continuous	167–189
Canadian Twin Otter	15 Jun–6 Jul	1000–1200	166–169, 171–176, 178, 180, 182, 184, 186–187
USU Seneca Piper II	16 Jun–8 Jul	0800–1500	167, 168, 174, 182, 184, 186–189
Sodar/lidar	14 Jun–9 Jul	0600–1400	166–184, 188–190
Balloon soundings	14 Jun–9 Jul	1–4 soundings	166–158, 172–184, 189–190

and flying over the Twin Otter transects and METFLUX tower sites at ~2100 m AGL.

3. Data description

Sensors from both the SMACEX and SMEX02 projects that are relevant to the research results presented in this issue are briefly described here. For additional details of the combined SMACEX–SMEX02 field campaigns see Kustas et al. (2003). A more thorough overview of the SMEX02 campaign and associated research results appear in a special issue of *Remote Sensing of Environment* (Njoku et al. 2004).

a. Satellite remote sensing data

Data from the AMSR-E instrument (details available online at http://wwwghcc.msfc.nasa.gov/AMSR/) launched in May 2002 were acquired. The lowest frequency is 6.9 GHz (C band), and, along with 10.7 GHz (X band), provides the best possibility in the near term for soil moisture estimation.

The Special Sensor Microwave Imager (SSM/I) satellites have been collecting global observations since 1987. The SSM/I satellite 19.4-GHz data can only provide soil moisture estimates under very restricted conditions because the frequencies were not selected for land applications. However, SSM/I data are useful in soil moisture algorithm development, serving as a prototype of the data stream that AMSR will provide and providing a cross reference to equivalent channels on the AMSR instrument. SSM/I data are freely available to users online (available at http://www.saa.noaa.gov/).

The National Aeronautics and Space Administration (NASA) *Terra* spacecraft (information available online at http://terra.nasa.gov/About/) includes several instruments of value to the soil moisture and land–atmosphere investigations. Of particular interest are the Moderate Resolution Imaging Spectroradiometer (MODIS) and Advanced Spaceborne Thermal Emission and Reflection Radiometer (ASTER). MODIS has a repeat cycle of 1–2 days, and with the recent launch of *Aqua* (in May 2002), permits up to two observations per day (morning and afternoon), with 250-m pixel resolution in the visible and near-infrared and 1 km in the thermal infrared. ASTER has 15-m resolution in the visible and near-infrared and 90 m in the thermal infrared. ASTER observations must be requested, and potential coverage is limited by the satellite track and repeat cycle.

The Landsat Thematic Mapper (TM) also provides high-resolution visible and near-infrared data (30 m) and thermal-infrared resolutions from 60 (Landsat 7) to 120 (Landsat 5) m. A description of the Landsat program and data can be found online (http://geo.arc.nasa.gov/sge/landsat/landsat.html). Both the IA and WC study sites fall in the area overlapped by two adjacent Landsat images, thus, permitting 8- versus the typical 16-day coverage. This resulted in nearly weekly coverage with Landsat.

The Geostationary Operational Environmental Satellite (GOES) provides near-continuous (15 min) monitoring in selected visible and thermal-infrared channels. The visible resolution is 1 km and thermal infrared is 4 km. The near-continuous observational capability of GOES permits daily monitoring of land surface states, except in overcast conditions.

During the SMACEX field campaign, sky conditions permitted acquisition of a Landsat-5 scene on 23 June (DOY 174), and Landsat 7 on 1 July (DOY 182) and 8 July (DOY 189). MODIS data, having useable scenes for most of the study area, include 16, 23, 24, 28–30 June, and 1 and 8 July (DOY 167, 174, 175, 179–182, and 189). For GOES, clear-sky morning periods are primarily used for modeling purposes, and days having cloud-free conditions in the morning included 16, 23, 27, 28, 30 June, and 1–2 July (DOY 167, 174, 178, 179, 181–183).

b. Aircraft remote sensing data

Aircraft remote sensing included visible, infrared, and microwave instruments. (Details of all the various instrumentation flown on the aircraft can be obtained from the following Web site: http://hydrolab.arsusda.gov/smex02/.) Only the instruments that are most directly applicable to the both projects will be briefly described here.

Shortwave imagery was acquired using Nikon[1] digital cameras with Thematic Mapper filters and a thermal-infrared Inframetrics camera on board the USU twin engine Seneca Piper II. Missions involved systematic coverage of the WC research area with a combination of shortwave (~1.5 m resolution) and thermal-infrared (~6 m resolution) measurements to coincide with airborne microwave flights. Flights were also conducted over the Twin Otter transects coincident with the Twin Otter missions. Missions for the mapping of the WC study area occurred on 16 June (DOY 167), and 1 (DOY 182) and 8 July (DOY 189). Other days having flights covering Twin Otter transects and METFLUX towers are listed in Table 1.

[1] The mention of trade names or commercial products in this article is solely for the purpose of providing specific information and does not imply a recommendation or endorsement by the U.S. Department of Agriculture.

Microwave instruments for evaluating soil moisture algorithms and mapping included the Polarimetric Scanning Radiometer (PSR) and the Passive and Active L and S (~2.7 GHz) band (PALS) instrument. The PSR is an airborne microwave imaging radiometer operated by the National Oceanic and Atmospheric Administration (NOAA) Environmental Technology Laboratory for the purpose of obtaining spatial maps of polarimetric microwave emission. Several of its microwave channels are similar to those of AMSR-E and, therefore, provide critical validation information. The PSR was flown on the NASA Wallops Flight Center P3-B aircraft, which flew transects over both the IA and WC study areas.

The PALS provides single-beam observations at L and S bands, and is dual polarized, and passive and active simultaneously (radar is polarimetric). As a result of the dual polarization, off-nadir viewing typical of conical scanning systems, and multifrequency and both active and passive observations, this instrument offers many interesting opportunities for both algorithm development and evaluation that have not been previously available. The PALS instrument flew on the National Center for Atmospheric Research C-130, which sampled the WC study area.

c. Ground-based remote sensing data

Radiometric temperature observations above and below the canopy were made at 12 of the 14 METFLUX tower sites using Apogee thermal-infrared radiometers (Apogee Instruments, Inc., model IRTS-P) having a nominal 60° field of view. Data were collected continuously throughout the study period. Above-canopy radiometric surface temperature was measured with a nadir view angle at nominally 2 and 5 m AGL, while below-canopy temperatures of the soil surface were measured at a ~45° view angle at 0.10 and 0.3 m AGL in soybean and cornfields, respectively.

Several ground-based atmospheric sensing systems were deployed for investigating the role of land surface heterogeneity on atmospheric properties and processes. The Raman scanning lidar sensor from LANL provided near-continuous water vapor concentration fields in the lower boundary layer, and a scanning wind lidar from UI provided horizontal winds throughout the boundary layer. A scanning elastic lidar, also from UI, mapped winds in the area, the boundary layer height, entrainment zone properties, and cloud information. A sodar and radar–radio acoustic sounding system (RASS) from LANL were used to measure ABL profiles of wind speed and direction and virtual temperature, respectively. This atmospheric sensing system was positioned along a boundary between adjacent corn- and soybean fields with two METFLUX towers located in fields 15 and 16 (Fig. 4).

d. Meteorological-flux tower measurements

The network of METFLUX tower observations was a key component of the SMACEX project. Towers were located in fields used for soil moisture and vegetation sampling during SMEX02–SMACEX. For each site, the ground cover of the crop, row width and orientation, instrumentation, latitude and longitude, and mode of collection during the field campaign is listed in Table 2. Fourteen CSAT3 sensors (Campbell Scientific, 3D sonic anemometer) and 10 LI7500 (LI-COR, CO_2/H_2O analyzer) were used. This gave the ability to place 10 EC systems throughout the WC domain to collect time series (high frequency) data of wind (u, v, and w components), sonic temperature, water vapor, and CO_2 from the LI7500. The remaining four CSAT3 sonic anemometers were used with KH20 sensors (Campbell Scientific, 1D krypton hygrometers/H_2O sensors) to provide the same data as above, except for CO_2. Thus, all 14 METFLUX towers provided momentum flux/shear velocity (u_*), sensible heat (H), and latent heat (LE) fluxes, with a subset of 10 also providing the CO_2 flux.

Each of the EC systems (CSAT3 with either LI7500 or KH20) used a Campbell 23X datalogger to execute the time series commands. The EC systems were sampled at 20 Hz. Twelve EC systems had a Libretto (Toshiba) 30, 50, or 70 minicomputer to store all of the raw high-frequency data in "time series mode." Each minicomputer had a Personal Computer Memory Card International Association (PCMCIA) card of either an 80- or 128-MB storage capacity. Approximately every 24 h the PCMCIA cards were exchanged at each EC tower with new PCMCIA cards. At this time, input location channels of the EC components were viewed online and inspected for instrument performance and instantaneous data integrity. If the EC systems were performing without error, normal time series acquisition was resumed with no loss of data. If a problem was encountered, it was solved and noted in field logbooks, and data acquisition resumed. The two remaining EC systems ran in "flux mode," with 30-min final output of the fluxes and statistics being stored on a 23X.

All EC systems were operating by 16 June (DOY 167), running in flux mode for several days to immediately diagnose any instrument malfunctions. The 12 EC systems were switched over to time series mode by 20 June (DOY 171), and were left in this mode until the end of the intensive field campaign on 9 July (DOY 190). The EC instruments were positioned on the towers to maintain nominally a 2-m height above the tops

TABLE 2. Description of METFLUX tower field sites located within the WC experimental domain. Information listed includes cover crop, row direction, row spacing, data collection mode, water vapor and/or CO_2 sensor, net radiometer model, and reference coordinates. Crop: C = corn, S = soybean; row direction: N = north–south, E = east–west, X = flex coil.

Field WC number	Crop	Row direction	Row spacing (m)	Flux (F) or time series (T) mode	LI7500 or KH20	CNR1 or REBS	Latitude (°)	Longitude (°)
03	S	N	0.38	T	LI7500	CNR1	41.983 809 85	−93.754 973 16
06	C	N	0.76	T	LI7500	CNR1	41.932 895 79	−93.753 315 02
10	S	X**	0.05	F	KH20	REBS	41.976 596 11	−93.691 093 44
11	C	N	0.76	F	KH20	REBS	41.9746	−93.693 69
13	S	N	0.76	T	KH20	REBS	41.952 153 01	−93.687 662 57
14	S	X	0.05	T	LI7500	REBS	41.945 984 67	−93.696 221 39
151*	C	E	0.76	T	LI7500	REBS	41.937 818 24	−93.663 131 8
152	C	E	0.76	T	LI7500	CNR1	41.937 815 42	−93.664 699 65
161	S	E	0.25	T	LI7500	REBS	41.934 141 03	−93.662 703 04
162	S	E	0.25	T	Li7500	CNR1	41.935 483 68	−93.664 058 39
23	S	E	0.20	T	KH20	REBS	41.992 453 28	−93.535 818 04
24	C	N	0.76	T	LI7500	CNR1	41.992 912 98	−93.528 578 74
25	C	E	0.76	T	LI7500	CNR1	41.942 268 63	−93.539 374 28
33	C	E	0.76	T	LI7500	CNR1	41.975 341	−93.644 312 94

* Fields WC 15 and 16 contained two METFLUX towers, which were designated as either tower "1" or "2."

** X represents flex coil planting, which has a very narrow row spacing/plant density and, thus, no well-defined row direction/orientation.

of the canopy. For the soybean fields the EC sensors remained static at ~2 m AGL during the field experiment, whereas the EC sensors over the cornfields were moved around at the end of June (DOY 180), from nominally 3 to 4 m AGL.

Ancillary measurements included energy balance components, net radiation (Rn), and soil surface heat flux (G). To estimate G, soil heat flux across the heat flow transducer (Gt) and heat transfer of the soil layer above the transducers (i.e., the storage term, estimated using soil temperature probes) were combined, so that $G = \mathrm{Gt} + S$. Mean air temperature and relative humidity, converted to water vapor pressure, were collected at all sites; near-surface soil moisture, using a heat capacity probe, was collected at 12 of the 14 sites, as was the surface temperature, from thermal-infrared radiometers described above.

For the 12 sites in the time series mode, ancillary measurements were made using a Campbell 21X datalogger connected to a Campbell AM 25T multiplexer. The two remaining sites running in flux mode had a 23X datalogger to collect both the ancillary and flux measurements. The ancillary measurements were sampled at 0.1 Hz or 10 s, with a 10-min-averaged output.

Net radiation was made using primarily one of two Rn sensors—the Kipp & Zonen CNR1 or the Radiation and Energy Balance (REBS) Q*7 series. There were seven CNR1 and seven REBS in the study. Priority levels were assigned to the METFLUX sites to ensure that the highest priority sites had the "A" suite of instruments, namely, the CSAT3 with LI7500 and a CNR1 net radiometer. For the sites with the CNR1 net radiometer, all four radiation components were recorded—incoming and outgoing short- and longwave radiation. These radiometers were positioned near the top of the METFLUX towers, ~3 m AGL over the soybean and ~5 m AGL over the cornfields. Soil heat flux Gt was measured using REBS the soil heat flow transducer (model HFT3) buried at 0.06 m, and the soil temperature probes of the soil layer above the HFT3 sensors for estimating S were made using Type-T soil thermocouples assembled by NSTL; these were buried at a depth of 0.02 and 0.04 m. Mean air temperature and vapor pressure measurements were made using a Vaisala temperature/RH probe (model HMP35C) enclosed in a radiation shield. These were mounted nominally at 1.5 m AGL over soybean and 2.5 m AGL over cornfields. The near-surface soil moisture measurements were made with a Stevens–Vitel Hydra probe installed at a depth of 0.05 m (with an effective sampling depth between 0.03 and 0.07 m).

e. Meteorological-flux aircraft measurements

Sixteen project flights with the Canadian Twin Otter flux aircraft were conducted during the period from 15 June to 6 July (DOY 166–187). As mentioned above, u_*, H, LE, CO_2, and ozone flux were measured at 40 m AGL on repeated passes over six tracks ranging in length from 5.7 to 12.2 km. Most flights included at least two soundings to profile the atmosphere from ~20 m AGL to about 300 m above the top of the mixed layer. A flight mission was approximately 2 h in duration, covering the various transects for the period between

1000 and 1200 central standard time (CST). Raw data were recorded at 32 Hz.

Three temperature probes were in operation on the Twin Otter during SMACEX, including an unheated fast-response Rosemount 102EAL temperature probe mounted on the port side of the nose and two 102DJ1CG heated probes, with one on each side of the nose. Dewpoint temperature was measured using an E, G, and G Model 137 Cambridge dewpoint sensor mounted on the starboard side of the Twin Otter nose. Dewpoint temperatures were also derived and recorded from the H_2O data measured by the two LI-COR CO_2/H_2O analyzers on the aircraft.

One of the long-standing policies for the instrumentation system on the Twin Otter is that most parameters are measured by at least two separate instruments. Thus, the aircraft carried two LI-COR CO_2/H_2O analyzers (LI-COR LI-6262). In early 2002, one was replaced with a new LI-COR LI-7000 unit, which features improvements in both accuracy and frequency response. During SMACEX, the LI-7000 was set for a 10-Hz response for the first five flight missions, and then 20 Hz for the remaining flights. This change did not seem to make an appreciable difference in the resulting signals.

Incident solar radiation and reflected solar radiation longwave radiation were measured with Kipp & Zonen CM-11 pyranometers with a 305–2800-nm spectral range. Radiometric surface temperature was measured on the Twin Otter for SMACEX by a Heitronics KT-19 infrared pyrometer with an approximately 3° field of view.

Prior to SMACEX, there was no direct measurement of Rn on the Twin Otter. Rather, it was calculated using the measured incident and reflected solar radiation with longwave contributions derived from the KT-19 surface temperature and air temperature. For SMACEX, a Kipp & Zonen CNR-1 net radiometer measured Rn, housed in a specially modified port wingtip. A comparison made with Rn data from six METFLUX towers closest to the Twin Otter flight tracks indicated that the CNR-1 gave better agreement with the tower observations than when computed indirectly, and, thus, has been used in the summary and archive files.

For SMACEX, the Twin Otter carried both an upward- and downward-looking Skye Industries Vegetation Greenness Indicator, which measures a ratio of near-infrared (730 nm)-to-red (660 nm) radiation. The downward reading can be correlated with the density of green vegetation beneath the aircraft. The upward-facing unit was installed to allow for a possible normalization of the downward reading to remove small changes that are seen in past projects associated with the variations in total solar radiation, such as those encountered in the shadows of clouds.

A downward-looking Exotech 100BX Satellite Simulator was mounted within the port wing of the Twin Otter. This simultaneously measures reflected radiation over four wavelength bands configured to simulate two Landsat TM visible and near-infrared bands for SMACEX.

4. Field conditions during SMACEX

During the SMACEX study period the corn and soybean crops grew rapidly. Observations near METFLUX towers indicated canopy heights starting at nominally 0.15 and 0.75 m, for the soybean and corn, respectively, and reached heights of ~0.5 and 2 m by mid-July. With such dramatic increases in vegetation height there were also significant increases in vegetation biomass and LAI.

Detailed vegetation-sampling data were collected on a weekly basis for METFLUX tower and soil moisture–sampling sites within the WC study area. Analyses by Anderson et al. (2004) indicate that LAI sampling in mid-June had an LAI of ~0.5 for soybean and ~1 for corn, and by mid-July LAI sampling yielded values on the order of two and four for soybean and cornfields, respectively. However, there was a fairly wide range in LAI values, particularly for corn, resulting from soil moisture variations across field sites that were caused by microtopographic and soil textural variations. This dramatic temporal change in the amount of plant cover and its spatial variability is illustrated in a sequence of LAI maps (Fig. 5) generated from the USU aircraft and Landsat TM remotely sensed data, using vegetation index–LAI relationships developed by Anderson et al. (2004). Despite a lack of precipitation for much of the project period (see below), there was vigorous growth by corn and soybean over the duration of the experiment.

Precipitation during SMACEX occurred a few days prior to 15 June (DOY 166), with a minor rainfall event (generally 0–5 mm being recorded) on 20 June (DOY 171). This was followed by a rain-free period for the WC area until 4 July (DOY 185). However, only some areas of WC received rain from this event and several other localized storms that occurred over the next 3 days. The rainfall distribution from the WC watershed rain gauge network for the precipitation events during SMACEX are illustrated in Fig. 6. A more widespread rain event occurred on 10 July (DOY 191), post-SMACEX campaign, where over 60 mm was recorded by the WC watershed rain gauge network, with similar amounts measured over the IA region. The rainfall events prior to, during, and immediately following the

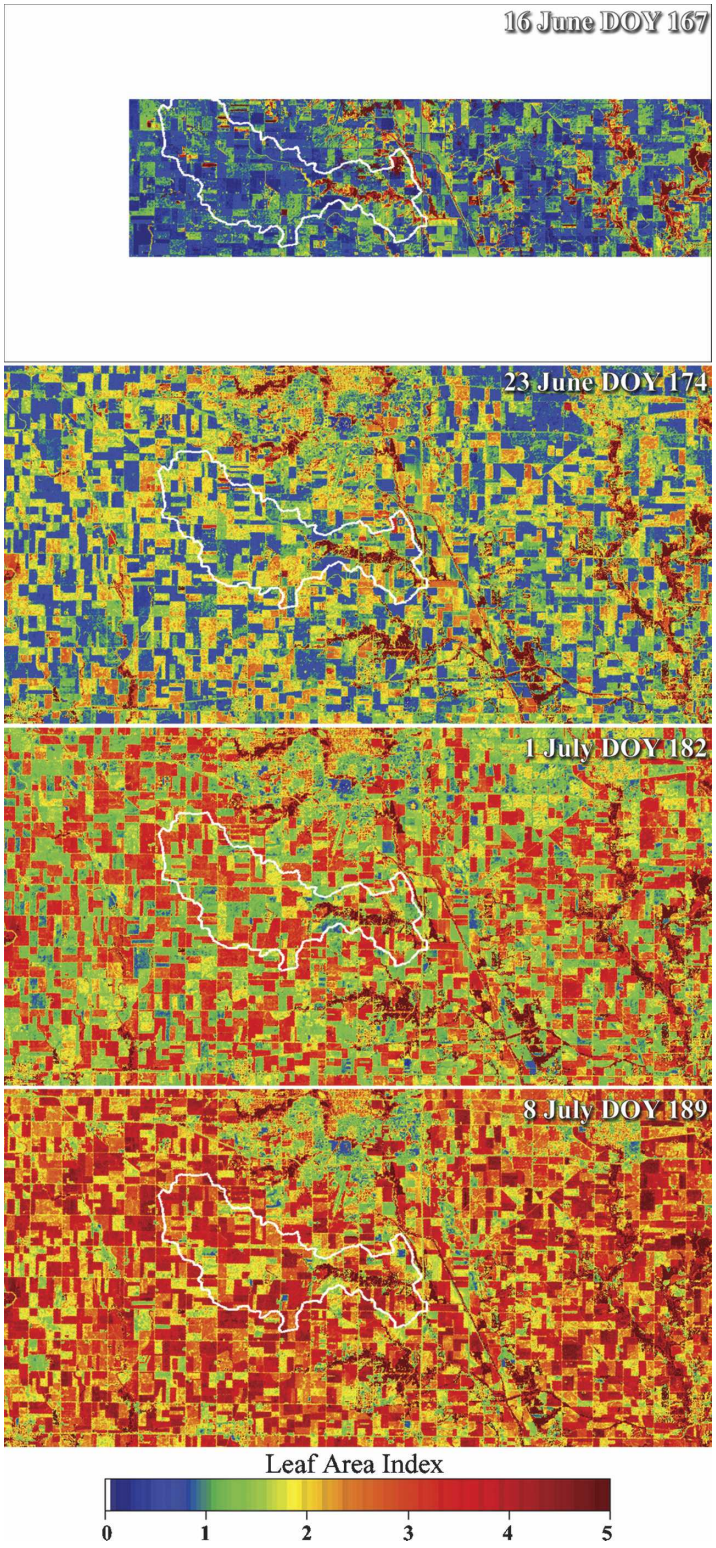

FIG. 5. LAI mapped at 30-m resolution for the WC study area derived from vegetation index–LAI relationships developed by Anderson et al. (2004). The remote sensing data are from the USU aircraft for 16 Jun (DOY 167), *Landsat-5* for 23 Jun (DOY 174), and *Landsat-7* for 1 Jul (DOY 182) and 8 Jul (DOY 189). The WC watershed boundary is delineated in white.

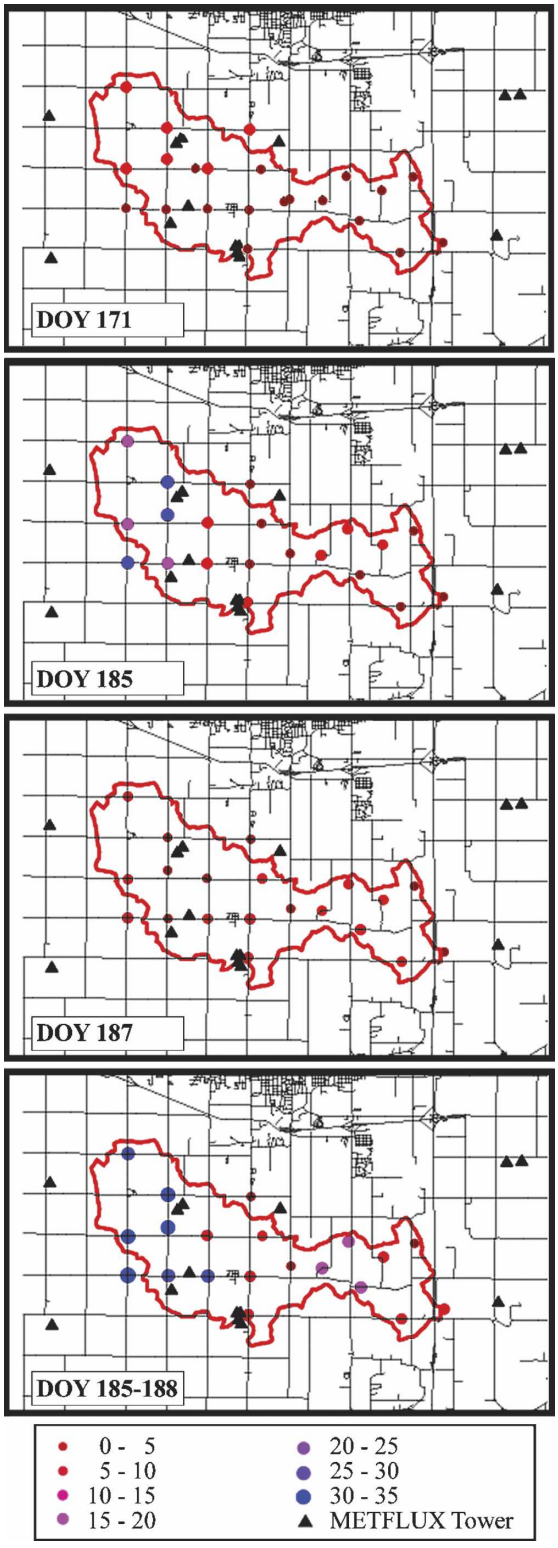

FIG. 6. The spatial distribution of rainfall amounts (mm) from events on 20 Jun (DOY 171), and 4 (DOY 185), and 6 (DOY 187) Jul, and total rain for the period 4–7 Jul (DOY 185–188). WC watershed boundary is delineated in red.

SMACEX campaign resulted in the surface soil moisture (0–5-cm depth) decreasing from the near-field capacity of ~25%–30% in mid-June to ~5%–10% before the rains, and then returning to near-field capacity in the upper soil layers, particularly after the rainfall event on 10 July (DOY 191).

Although the available surface moisture decreased considerably, METFLUX tower measurements indicated that LE and CO_2 fluxes generally increased while H decreased, initially, then remained fairly constant, until again decreasing near the end of the field experiment. This resulted in the Bowen ratio (BR = H/LE) generally decreasing from ~0.5 and 1 for corn and soybean, respectively, at the start of SMACEX, to ~0.2 and 0.5 for for corn and soybean, respectively, before the rains near the end of the study period. Similar trends were obtained with the aircraft-based flux observations. In addition, there was a significant reduction in soil heat flux as the canopy cover increased from ~50% to nearly 100% by the end of SMACEX.

Near the end of the rain-free period visual signs of water stress were evident at some field sites, which contributed to the wide range in LAI values that were observed in mid-July and even greater variability in the analysis of the USU aircraft imagery (Anderson et al. 2004). This dry condition caused slight increases in BR values in both the METFLUX tower and aircraft-based measurements before the rains.

5. Overview of preliminary findings

The research results presented in this issue can be divided into three broad categories. One category (group of papers) uses the observational data to understand the influence of land surface properties (e.g., vegetation type, soil texture, microtopography) and states (e.g., soil moisture, fractional vegetation cover and/or biomass, surface temperature) on soil–vegetation–atmosphere exchanges and in affecting remote sensing algorithms used estimating these states. Another validates remote sensing–based soil–vegetation–atmosphere transfer (SVAT) model output and evaluates any related effects of landscape properties on remote sensing–based SVAT parameterizations. The third evaluates the utility of using remote sensing data and/or remote sensing–based SVAT output, in combination with more traditional SVAT schemes, that simultaneously solve for water and energy fluxes driven by hydrometeorological inputs (i.e., precipitation, solar radiation, wind, and air temperature/vapor pressure).

In the first category, Prueger et al. (2005) evaluated the temporal and spatial variability in energy and CO_2 fluxes from METFLUX tower systems and from the

Twin Otter aircraft. During this period of rapid growth in corn and soybean crop cover, the heat, water vapor, and carbon dioxide fluxes show the greatest spatial and temporal variability between crops; however, there was also some significant variation among the same crop because of crop cover/biomass variation. These differences were determined to be statistically significant using an analysis of uncertainty in the EC measurements from instrument intercomparison studies conducted before and after the field campaign (Meek et al. 2005). The network average fluxes were in good agreement with area-averaged measurements from the aircraft. The largest discrepancy was in the latent heat flux with the largest differences correlated to a case where either the METFLUX or aircraft system had poor closure in the surface energy balance.

Parkin et al. (2005) evaluated soil respiration over the WC study area using chamber measurements and found that the field respiration rates were not significantly affected by landscape position (i.e., summit, side slope, and depression). Laboratory measurements gave the opposite results; however, crop roots did not affect the laboratory measurements. The chamber measurements showed a significant crop effect on soil respiration values. Approximately half of the nighttime CO_2 exchange was the result of respiration from plant shoots and leaves, while the other half was a result of soil respiration. Not accounting for these differences can lead to significant bias in net CO_2 exchange measured by METFLUX towers, and would certainly be exacerbated when estimating regional-scale net primary production.

Kustas et al. (2005) used the METFLUX tower and Twin Otter measurements to estimate local- and regional-scale aerodynamic roughness length. A procedure for the aggregation of local roughness values from the different land cover types based on blending-height concepts yielded effective surface roughness values that were from ~1/2 to 1/4 the magnitude estimated with the aircraft data. This indicated additional kinematic stress caused by form drag from isolated obstacles (i.e., trees, houses, and farm buildings), and the interaction of adjacent corn- and soybean fields are probably important factors affecting the effective surface roughness length for this landscape. Further supporting this result was the comparison of shear velocity u_* measurements from the towers versus the aircraft, which indicated that u_* from aircraft was 20%–30% higher, on average. In addition, u_* over corn was 10%–30% higher than that over soybean, depending on stability. The affect of underestimating the regional roughness on sensible heat flux estimation using surface–air temperature differences was relatively minor; a 50%–75% underestimate caused only a 10%–15% underestimate in H, respectively.

Eichinger et al. (2005) used the vertically staring elastic lidar, providing a continuous record of the boundary layer height and the height and thickness of the entrainment zone, and atmospheric balloon soundings to estimate the surface sensible heat flux using the Batchvarova–Gryning boundary layer model. Flux estimates made over 6 days were compared to METFLUX tower measurements. The average root-mean-square difference between modeled and measured H was less than 25 W m^{-2}. The combined measurement–modeling technique provides a unique ground-based remote sensing approach for estimating regional-scale H, which is also independent of surface boundary conditions that are used by SVAT schemes. Consequently, this approach provides an independent regional-scale H estimate to compare with SVAT output. A sensitivity analysis of key model inputs indicated that uncertainty in the potential temperature gradient above the boundary layer might result in a significant error in flux computations.

Wen et al. (2005) evaluated the potential of soil moisture and vegetation water content estimation from SSM/I brightness temperatures. The sensitivity between brightness temperature and soil moisture rapidly decreased with increasing plant water content. However, the SSM/I brightness temperatures showed a response to soil moisture after rainfall events, due, in part, to thermal effects, whereby the soil and vegetation temperatures would be significantly lower after a rainfall. The comparison of retrieved soil moisture with the regional sampling indicated absolute errors on the order of 5% volumetric soil moisture were achieved over a 3-week study period, but the accuracy is highly dependent on the level of vegetation effects and atmospheric precipitable water.

McCabe et al. (2005) compared AMSR-E soil moisture retrievals with those produced using a land surface microwave emission model (LSMEM) driven with data from the North American Land Data Assimilation System (NLDAS), and MODIS land cover products. Soil moisture retrievals from the AMSR-E X-band sensor were evaluated with a network of ground soil moisture samples and higher-resolution estimates from the airborne PSR C-band data, which provided information on the AMSR-E subpixel variability. The results indicate that absolute errors of less than 5% volumetric soil moisture are achievable with AMSR-E X-band sensor using the LSMEM. This finding indicates a potential for estimating surface soil moisture patterns at regional scales, even in the presence of relatively dense nonforested vegetation cover.

The second category of remote sensing–based SVAT

(RS-SVAT) validation and algorithm assessments includes a paper by Li et al. (2005), evaluating two resistance network formulations used in the two-source model (TSM) for estimating soil and canopy energy exchanges. The parallel resistance formulation does not consider interaction between the soil and canopy systems, whereas the series resistance algorithm provides interaction via the computation of a within-air canopy temperature. This temperature represents the effective source height for heat exchange between the soil–canopy system and the overlying atmosphere. Satellite and aircraft remote sensing observations of radiometric surface temperature and fractional vegetation cover were used with METFLUX tower observations for evaluating the parallel and series resistance networks. The largest discrepancy with METFLUX tower observations was in model output of H ($\approx$35%), but did not cause significant differences in LE ($\approx$10%). This is a result of the fact that for most of the experimental period, LE fluxes were 2–5 times larger than H. Although both series and parallel versions of TSM gave similar results, the parallel resistance formulation is shown to be more sensitive to model parameter specification, particularly in accounting for effects on flux partitioning resulting from vegetation clumping via row crop planting. A sensitivity analysis also indicated that the parallel resistance network is more sensitive to errors in vegetation cover estimation. This greater sensitivity with the parallel model appears to be related to the neglect of moderating effects associated with the computation of a within-air canopy temperature by the series resistance network.

Anderson et al. (2005) evaluated the effects of nonrandom vegetation cover on surface flux estimation using TSM, the same RS-based SVAT described by Li et al. (2005), but coupled to a regional ABL growth model using the temporal change in GOES radiometric surface temperature; it is called the Atmosphere–Land Exchange Inverse (ALEXI) model. The 5-km regional output was disaggregated to Landsat TM resolution using a scaling method called DisALEXI. A procedure to quantify row-scale clumping in corn- and soybean fields was developed. These derived clumping indices were used to represent subpixel clumping in Landsat cover estimates at 30-m resolution, which were then aggregated to estimate clumping at the 5-km scale of the regional model, reflecting field-to-field variations in vegetation cover amounts. Vegetation clumping affects the relationship between surface temperature and LAI/fractional vegetation cover inputs, and resulted in significant improvement between model flux output and METFLUX tower and Twin Otter measurements. Clumping is likely to play an important role in many remote sensing–based SVAT models because it fundamentally affects the relationship between surface temperature and vegetation cover.

Su et al. (2005) evaluated another RS-based SVAT model called the Surface Energy Balance System (SEBS) using the continuous radiometric surface temperature observations from the METFLUX towers and the METFLUX tower energy balance measurements. Agreement between SEBS estimates and METFLUX observations of LE were generally within 15%, although there were larger discrepancies, particularly at some of the soybean sites that had sparse and heterogeneous canopy cover. The SEBS model was also applied to a Landsat image with a coarser-resolution radiation product from GOES, an albedo product from MODIS, and meteorological forcing from NLDAS. The comparison with METFLUX tower estimates indicated greater scatter, particularly for the soybean sites. Possible factors causing this result for the soybean sites include incorrect parameterizations, emissivity effects and mismatch in the scale of the radiometric surface temperature observations, and the source area contributing to the METFLUX tower measurements.

The issue of model validation with tower flux observations is considered in detail by Chávez et al. (2005) using an RS-based SVAT with an in situ calibrated surface temperature–aerodynamic temperature algorithm. The resulting heat flux images were integrated using 2D heat flux source area models (footprint models) and were compared to METFLUX tower measurements. The footprint integration models that were tested indicate that they perform better than simple averaging of upwind pixels from the METFLUX tower. This simple pixel averaging is typically the procedure adopted in SVAT model validation studies (as is the case of the papers in this issue). Further studies should be directed to test the footprint model predictions for heterogeneous surfaces under a wider range of atmospheric and surface conditions.

In the third category, the paper by Crow et al. (2005) examined the two basic types of SVAT approaches—the RS-SVAT, where remotely sensed boundary conditions drive model calculations (diagnostic approach), and a combined water and energy balance SVAT (WEB-SVAT) that continuously simulates water and energy exchanges driven by hydrometeorological observations (predictive or prognostic approach). The TSM is the RS-SVAT output, used as a comparison to fluxes from the WEB-SVAT, called the "TOPMODEL"-based Land–Atmosphere Transfer Scheme (TOPLATS). Both TOPLATS and TSM fluxes were compared to the METFLUX tower measurements, showing similar agreement in LE with root-mean-

square (rms) errors of around 65 W m^{-2}, but with significantly less agreement for TOPLATS relative to TSM for *H*, with rms errors of approximately 45 and 20 W m^{-2}, respectively. Intercomparisons of the spatial patterns in the TSM and TOPLATS fluxes indicated that the TOPLATS model tended to overpredict contrasts in fluxes between corn and soybean. It is shown that model flux differences with the observations are sufficiently independent, and, thus, may provide opportunities for improving the reliability in the spatial output of both schemes through data assimilation and model updating/calibration.

These research results have made progress in addressing components of research areas in the mainstream of current national and international interests in hydrometeorology. These include developing remote sensing techniques to provide the robust estimation of heat, water vapor, and carbon dioxide fluxes at multiple scales, improving the understanding of the role of the soil–vegetation dynamics on atmosphere interactions, and beginning to develop methods for using new types of atmospheric/hydrologic observations or remotely sensed data products for improved SVAT predictions. Key applications of SVAT model predictions of soil moisture and subsurface soil temperature states include the initialization of numerical prediction models and monitoring water availability for natural and agricultural ecosystems. Opportunities from both modeling and measurement/remote sensing applications for evaluating SVAT formulations and ultimately improving SVAT predictions of fluxes and soil moisture and temperature states are presented in this special issue.

Acknowledgments. Funding provided by NASA Grant NRA 00-OES-07 from the NASA Terrestrial Hydrology Program made the SMACEX project possible. Logistical support from the USDA-ARS National Soil Tilth Lab and the SMEX02 project were critical in the success of the SMACEX field campaign. The authors thank Dennis Lettenmaier and Wade Crow for their comments on earlier versions of this manuscript.

REFERENCES

Adegoke, J. O., R. A. Pielke Sr., J. Eastman, R. Mahmood, and K. G. Hubbard, 2003: Impact of irrigation on midsummer surface fluxes and temperature under dry synoptic conditions: A regional atmospheric model study on the U.S. High Plains. *Mon. Wea. Rev.,* **131,** 556–568.

Anderson, M. C., C. M. Neale, F. Li, J. M. Norman, W. P. Kustas, H. Jayanthi, and J. Chavez, 2004: Upscaling ground observations of vegetation cover and water content during SMEX02 using aircraft and Landsat imagery. *Remote Sens. Environ.,* **92,** 447–464.

——, J. M. Norman, W. P. Kustas, F. Li, J. H. Prueger, and J. R. Mecikalski, 2005: Effects of vegetation clumping on two-source model estimates of surface energy fluxes from an agricultural landscape during SMACEX. *J. Hydrometeor.,* **6,** 892–909.

Chávez, J. L., C. M. U. Neale, L. E. Hipps, J. H. Prueger, and W. P. Kustas, 2005: Comparing aircraft-based remotely sensed energy balance fluxes with eddy covariance tower data using heat flux source area functions. *J. Hydrometeor.,* **6,** 923–940.

Crow, W. T., F. Li, and W. P. Kustas, 2005: Intercomparison of spatially distributed models for predicting surface energy flux patterns during SMACEX. *J. Hydrometeor.,* **6,** 941–953.

Eichinger, W. E., H. E. Holder, D. I. Cooper, L. E. Hipps, R. Knight, W. P. Kustas, J. Nichols, and J. H. Prueger, 2005: Lidar measurement of boundary layer evolution to determine sensible heat fluxes. *J. Hydrometeor.,* **6,** 840–853.

Hatfield, J. L., J. H. Prueger, and D. W. Meek, 1999a: Spatial variation of rainfall over a large watershed in central Iowa. *Theor. Appl. Climatol.,* **64,** 49–60.

——, D. B. Jaynes, M. R. Burkart, C. A. Cambardella, T. B. Moorman, J. H. Prueger, and M. A. Smith, 1999b: Water quality in Walnut Creek Watershed: Setting and farming practices. *J. Environ. Qual.,* **28,** 11–24.

Kustas, W. P., T. J. Jackson, J. H. Prueger, J. L. Hatfield, and M. C. Anderson, 2003: Remote sensing field experiments for evaluating soil moisture retrieval algorithms and modeling land-atmosphere dynamics in central Iowa. *Eos, Trans. Amer. Geophys. Union,* **84,** 485–493.

——, J. H. Prueger, J. I. MacPherson, M. Wolde, and F. Li, 2005: Effects of land use and meteorological conditions on local and regional momentum transport and roughness for Midwestern cropping systems. *J. Hydrometeor.,* **6,** 825–839.

Li, F., W. P. Kustas, J. H. Prueger, C. M. U. Neale, and T. J. Jackson, 2005: Utility of remote sensing–based two-source energy balance model under low- and high-vegetation cover conditions. *J. Hydrometeor.,* **6,** 878–891.

McCabe, M. F., H. Gao, and E. F. Wood, 2005: An evaluation of AMSR-E-derived soil moisture retrievals using ground-based and PSR airborne data during SMEX02. *J. Hydrometeor.,* **6,** 864–877.

Meek, D. W., J. H. Prueger, W. P. Kustas, and J. H. Hatfield, 2005: Determining meaningful differences for SMACEX eddy covariance measurements. *J. Hydrometeor.,* **6,** 805–811.

Njoku, E. G., V. Lakshmi, and P. E. O'Neill, 2004: Preface soil moisture field experiment special issue. *Remote Sens. Environ.,* **92,** 425–426.

Parkin, T. B., T. C. Kaspar, Z. Senwo, J. H. Prueger, and J. L. Hatfield, 2005: Relationship of soil respiration to crop and landscape in the Walnut Creek watershed. *J. Hydrometeor.,* **6,** 812–824.

Prueger, J. H., and Coauthors, 2005: Tower and aircraft eddy covariance measurements of water vapor, energy, and carbon dioxide fluxes during SMACEX. *J. Hydrometeor.,* **6,** 954–960.

Su, H., M. F. McCabe, E. F. Wood, Z. Su, and J. H. Prueger, 2005: Modeling evapotranspiration during SMACEX: Comparing two approaches for local- and regional-scale prediction. *J. Hydrometeor.,* **6,** 910–922.

Weaver, C. P., and R. Avissar, 2001: Atmospheric disturbances caused by human modification of the landscape. *Bull. Amer. Meteor. Soc.,* **82,** 269–281.

Wen, J., T. J. Jackson, R. Bindlish, A. Y. Hsu, and Z. B. Su, 2005: Retrieval of soil moisture and vegetation water content using SSM/I data over a corn and soybean region. *J. Hydrometeor.,* **6,** 854–863.